Seismic performance-based assessment of a RC pipe rack accounting for dynamic interaction

Luigi Di Sarno [a, b,*] and George Karagiannakis[a]

a University of Sannio, Piazza Roma, 21, 82100 Benevento, Italy

b University of Liverpool, Liverpool L69 3BX, UK

Abstract

In contrast with common buildings, the limit-state assessment has not been applied to pipe-rack – piping systems yet, albeit the seismic vulnerability of critical pipes is rather high. The current engineering practice may design pipe rack – piping systems in a risk-inconsistent way due to the conservative acceptance criteria of seismic codes that keep pipes in the elastic range. Additionally, the response of pipes could become complex when considering differential displacements between internal supports, pipe edges and adjacent structures, which static methods may not describe efficiently. The design of a typical RC pipe rack – piping system in a code-consistent way resulted in two main outcomes. First, the piping required the increase of structural members cross-section, and secondly, the differential displacement was the main reason of pipe failure both in the longitudinal (unrestrained) as well as transverse direction. Finally, the performance-based assessment of this type of system demonstrated that the spectral acceleration is mildly more efficient and sufficient intensity measure than ground ones to describe the damage on piping. The observed mean annual frequency of exceedance was 57% smaller than the targeted value for the pipes, whereas the difference was considerably higher for the pipe rack. This outcome corroborated

the conservativeness of codes and the risk-inconsistency between the structural and non-structural members.

Keywords: pipe rack; piping; dynamic interaction; seismic design; risk assessment; fragility; efficiency; sufficiency.

1. Introduction

Pipe Racks (PRs) or supporting structures are included in process plants and outfitted with critical piping that transfer hazardous substances from one unit to another for operational, maintenance and safety reasons. Process plants are continuously exposed to natural hazards, and the earthquake hazard that the present study addresses is rather crucial, since several accidents have been triggered in the past years ([1], [2]). Piping and pipework has been reported in [3] and [4] as the most risk prone equipment inside process plants, thus it requires special consideration during the design and analysis phase. Risk drivers of piping failure regarded human, organisation and mechanical aspects, but they were also related to the construction, layout and installation on PRs as well as interaction with adjacent structures during seismic events. For example, the field inspection of [5] on industrial facilities that experienced damage during the 2008 Wenchuan earthquake showed that both direct earthquake loading and falling debris from surrounding units caused piping failure. Concerning the former case, pipe severing was observed at pipe-to-equipment connection, pipe joints as well as pipe-to-pipe support due to Differential Displacements (DDs) (Fig. 1a) and rigidity of connection (Fig. 1b). Indeed, these are the two main reasons of piping failure due to earthquake-induced forces.

a) b)

Fig. 1 a. Failure at pipe joint connection due to differential displacement and b. pipe severing due to rigid connection [5]

An important aspect that characterises the seismic response of these systems, which should be addressed during the design phase, regards the dynamic interaction between equipment (piping, vessels, etc) and supporting structures. The European code for seismic design of structures [6] and piping [7], and the national ones e.g. the Italian design standard [8] along with the guideline document [9] stipulate that nonstructural elements can be analyzed by neglecting dynamic coupling with supporting structures. However, no particular reference to the aspects that necessitate the use of coupled case is made. This assumption may not be always safe enough. Also, the complexity of the system and the effectiveness of the formulae that are proposed by the codes for the estimation of equivalent static forces at pipe's level have not been examined sufficiently in the literature, particularly for industrial structures. For instance, [10] and [11] demonstrated that simplified approaches of codes for the seismic design of nonstructural components may considerably underestimate the peak acceleration demands, particularly when the supporting

structure has significant higher mode components. Overall, the degree of dynamic interaction depends on the rigidity of connections or type of Pipe Support (PS), the weight of supported equipment as well as the component damping that seismic codes do not take into account.

Furthermore, the design of piping is not in unison with modern design methods that account for nonlinearity of material, so that both structural and non-structural members are risk-consistent. Instead, stress-based methods are still adopted due to the additional margin of safety and the limitations of existing analysis software platforms. For example, [12] designed a piping system according to the stress-based method, and the strain on pipe at the Operating or Design Basis Earthquake (hereafter called OBE) level was roughly 2 times lower than the yielding one. Also, [13] illustrated that a code-conforming PR could be quite rigid resulting in very low Inter-story Drift Ratio (IDR) and pipe stress below yielding point even at Safe Shut-down Earthquake (SSE). The research on the nonlinear analysis of PR – piping systems is rather limited. For instance, [14] illustrated that flexible yet code-conforming PR configurations proved more beneficial for the response of pipes, since they lessened the Peak Floor Acceleration (PFA) demand; however, no coupling with pipes was accounted for in the analysis.

The response of piping is affected not only by the intensity of input acceleration at support level but also by the differential displacements within a rack or with adjacent structures. The differential displacement between a pipe support at ground and primary structure level was the main reason of failure for a nuclear piping system attached to a building structure [15], and thus peak ground measures e.g. peak ground acceleration and velocity did not correlate efficiently with the seismic response. This finding comes in contrast with the efficiency of former measures compared to underground pipelines (e.g. [16] among others). Peak ground and spectral measures have also been found efficient and sufficient for common civilian assets and bridges ([16], [17]).

Given that the seismic response of elevated pipes is affected by the dynamic characteristics of the PR and could become complex by virtue of differential displacements, it is important to examine the efficiency and sufficiency of different intensity measures. The present study intends to examine briefly several design aspects of a typical RC PR e.g. dynamic coupling and amplification factor at pipe's level, and then the PR is assessed probabilistically in the nonlinear range towards estimating and comparing the risk between structural members and piping.

2. Description of modelling and design of the case study

A long and short RC PR are part of a regasification plant and carry seven steel pipes that transfer liquified ethylene to and from a concrete storage tank (Fig. 2a). The ethylene is distributed to the nearby process units for regasification. Both PRs are located between the tank and the process units, and considering that ethylene is highly combustible and explosive, the PR is made of RC instead of steel to achieve higher fire resistance. In the framework of this study, only the short PR will be assessed, since it was demonstrated by [18] that the most critical pipe is located between the short PR and the tank (Fig. 2b). In this way, the computational cost reduces considerably.

2.1 Pipe rack – storage tank

The short PR is 6 meters long in the X direction, 9 meters long in the Y direction with 3 meters sub-spans at the top and rises at 8.3 meters above the ground level with an intermediate floor at 6 meters for future piping installation (Fig. 2c). The structural members were made of concrete class C40/50 and steel grade B500C was used for the concrete reinforcement. Several load combinations are commonly used for the dimensionalization of structural members for the serviceability and ultimate limit states, accounting for snow and wind loading. The earthquake scenario that the rack was examined for includes the self-weight of PR and pipes (G), the live load (Q) that regards the

additional weight due to future pipe installation and cable trays, and finally, thermal load, *TL*. The live load of pipes, Q_p, was subjected on transverse beams (bends) at +6.0 and +8.3 metres level (midline), and it was calculated at 0.8 kN/m. Furthermore, six cable lines accounting for 0.8 kN/m per each one (Q_p=4.8kN/m in total) run on the upper beams; however, the lower beams were subjected to the same load again due to future installation.

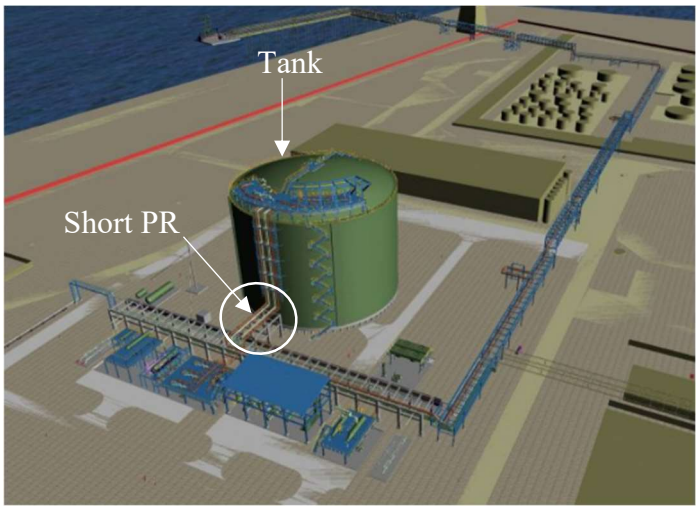

a)

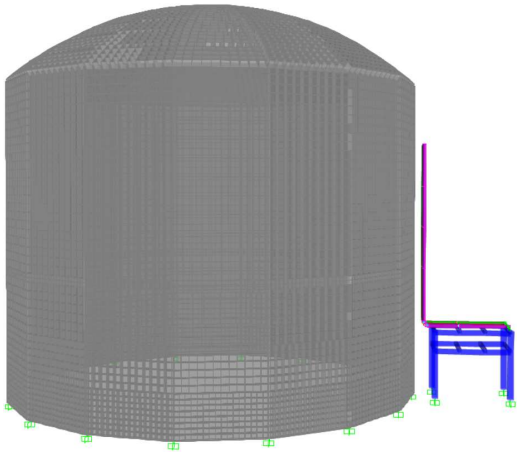

b)

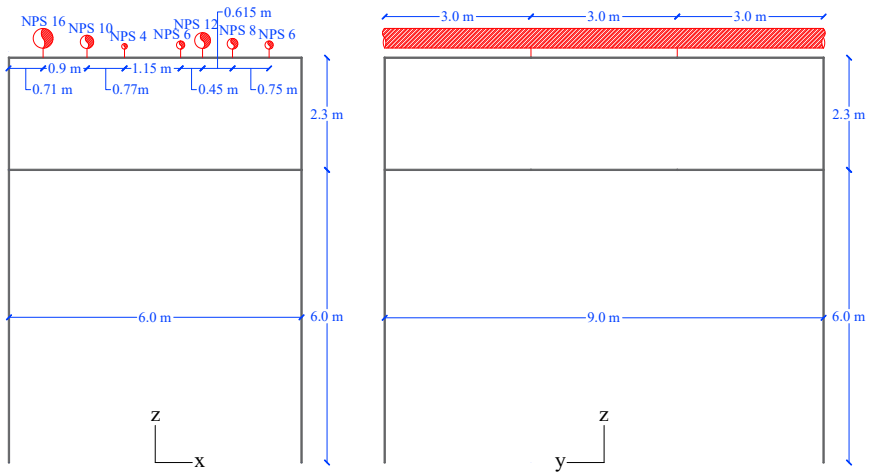

c)

Fig. 2 Ethylene terminal plant a. layout, b. the tail PR under examination, and c. the dimension of rack in both side planes

The PR was placed in a seismic prone industrial area (Priolo Gargallo, Sicily, Italy) and analysed using the response spectrum method considering usage class III (industrial facility that processes combustible substances) and 5% equivalent viscous damping in line with [8]. The return period, T_R, of earthquake occurrence, which [8] prescribes at 475 years, increased by the importance factor, C_U, of 1.5 to account for the higher risk of process plants. Thus, the return period of the design earthquake was estimated at 713 years, which refers to 6.8% probability of exceedance of Safe Life Limit State (SLLS) in 50 years or $1.4 \cdot 10^{-3}$ annual frequency of exceedance, assuming a Poisson distribution ([8]). The design peak ground acceleration (a_g) was estimated at 0.30g, and the Zero Period Acceleration (ZPA) rose at 0.39g, since soil type C (V_s=210 m/s) was assumed. Concerning the behaviour factor selection, no value is currently postulated in [8] and [6] for PRs. Considering that a behaviour factor should be selected in the following for the design of pipes as well, the minimum value between the factor prescribed in [8] for medium ductility RC resisting frames without irregularities (q_s=3.3) and the minimum value as estimated among the seven pipes (q_a=2) according to [19] was selected. A comparison between q factors prescribed in different seismic codes can be found in [13]. The main design parameters of PR are recapitulated in Table 1.

The storage tank serves to store ethylene at low temperature with a maximum capacity of 29,000 tonnes. The cylindrical shell is 38 m high with 24.5 m inner radius and 65 cm wall thickness. The tank dome has an average thickness of 600 mm and reaches an overall height of 47.4 m. Since the tank is full of containment, only the impulsive mass was considered and placed at 42% of total cylindrical height ([20]). The predominant period of the tank is equal to 0.31 sec.

Table 1: Modelling and design parameters for the PR for the SLLS

Location	Priolo Gargallo, Italy
Frame type	Moment resisting
Concrete	C40/50
Importance class	III
Return period	713 yrs (or 6.8% in 50 yrs)
$\mathbf{a_g}$	0.30 g
Soil type	C (V_s=210 m/s)
$\mathbf{q_{min}=min(q_s,q_a)}$	2
Live load Q_{k1}	5.6 kN/m

2.2 Piping system

The pipe schedule of six out of the seven pipes is (SCH10) and the Nominal Pipe Size ranges from 4" to 12". Only Pipe 1 (P-1) has pipe schedule 20 and NPS 16" (Fig. 2c). Furthermore, all the pipes are made of A312/TP304L steel with 0.2% proof stress equal to 250 MPa, elastic modulus of 204 GPa and 0.3 Poisson's ratio. The straight pipes and pipe bends were modelled with 2-node linear beam elements with hollow cross section; however, the bends (elbows) were discretized into 20 elements to achieve higher accuracy. This modelling configuration was verified by comparing the response of the 8 NPS bend (mean pipe diameter, D_m=216.33mm, and elbow radius, R=305mm) under bending and shear using beam and shell elements on [21]. More information about the elbow configuration and load application can be found in [22]. Apart from the pipe element type, the pipe-to-pipe support connection is of primordial importance for the seismic response. The type of pipe support depends on the piping layout and possible loading scenarios e.g. earthquake loads or thermal effects. For instance, when earthquake loads govern the response, it might be more suitable to support pipes in a more flexible manner by avoiding fixed connections

and introducing pipe loops ([18]). Also, rigid pipe-to-pipe rack connections can increase considerably the shear force on beams, as it was demonstrated by [23] and [24] for non-seismic code compliant pipe supports. Having said that, all the pipes were modelled to move freely in the longitudinal direction (Y) and restrained only in the transverse (X) and vertical one (Z).

Finally, the type of boundary conditions is another critical parameter that may alter significantly the response. In virtue of high computational cost and time constraints, the analysis is impossible to account for the entire length of piping; therefore, appropriate boundary conditions should be considered. First, the pipes that run along the height of the tank were supported at three different points (PS1, PS2 and PS3), and fixed at 81% of the total height of the tank shell (BC1(1-7)) (Fig. 3). PS3 was placed high enough on the tank to absorb differential displacements at the intersection with the PR. Also, the fixed point was considered deliberately to reduce the dead load of pipes. Finally, to avoid overstress at the edge of the pipes due to differential displacement of the PR with the tank, 6 springs (three translational and three rotational) were calibrated accounting for the flexibility of the pipes that run on the long rack in the X direction (see also Fig. 2a). For the sake of brevity, the type and coordinates of pipe supports are not quoted.

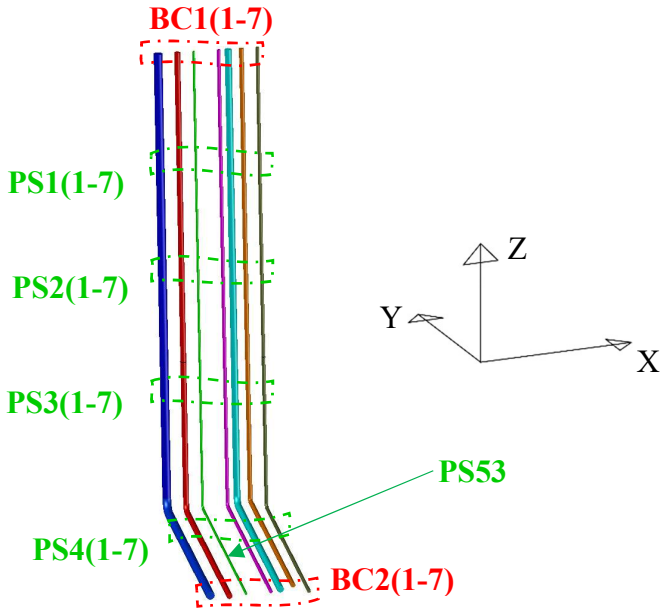

Fig. 3 Piping system layout as well as PS type, boundary conditions (BCs) and geometrical properties.

2.3 Dynamic coupling

Both European [6] and Italian [8] codes postulate that the analysis of nonstructural components can be conducted by neglecting dynamic coupling and considering an equivalent static force at pipe's level, which the current engineering practice espouses. In particular, the recent guideline [9] and [6] postulate that the seismic design force at a nonstructural component level should be calculated as follows:

$$F_a = \frac{S_e \cdot W_a}{q_a} AF_{1,2} \tag{1a}$$

$$AF_1 = \begin{cases} \left(1+\frac{z}{H}\right)\cdot\left[\frac{a_p}{1+(a_p-1)\cdot\left(1-\frac{T_a}{a\cdot T_1}\right)^2}\right], & T_a < a\cdot T_1 \\ \left(1+\frac{z}{H}\right)\cdot a_p, & a\cdot T_1 \le T_a < b\cdot T_1 \\ \left(1+\frac{z}{H}\right)\cdot\left[\frac{a_p}{1+(a_p-1)\cdot\left(1-\frac{T_a}{b\cdot T_1}\right)^2}\right], & T_a > b\cdot T_1 \end{cases} \quad AF_2 = \left[\frac{3\cdot\left(1+\frac{z}{H}\right)}{1+\left(1-\frac{T_a}{T_1}\right)^2} - 0.5\right] \tag{1b}$$

where S_e is the elastic spectral acceleration, W_a is the component weight, q_a is the component behaviour factor that is considered equal to 2 for piping (pipe with the greatest diameter has $r/t<100$, see also [19]), $AF_{1,2}$ is the amplification factor of the component as prescribed by [9] and [6], respectively, z and H are the component and total structural height, respectively, a_p, α and b are parameters given in [9] depending on the fundamental period of the structure, and finally, T_1 and T_a is the vibration period of the PR and component, respectively. It should be noted that the difference between the AF in [6] and [9] lies in the fact that the latter code considers different AF

based upon the rigidity of supporting structure as well as the period ratio between the structure and the component; the more rigid the structure or the closer the T_a/T_1 to unity is, the higher the *AF* is. The *AF* for both codes is evaluated in Section 3.5.

In contrast with engineering practice, the pipes are analyzed accounting for dynamic coupling with the PR. After ensuring the seismic integrity of the PR, the response of pipes was checked by analyzing the system with 3 spectrum compatible seismic records (Rec1-3), which is the minimum number for structural analysis, as prescribed in [6]. Time-history analysis is more rarely adopted with regard to other methods due to the high computational cost. Also, the allowable stress-based design method is commonly accounted for the pipes as a simple and conservative method that keeps them in the linear range for the design earthquake. To illustrate this conservativeness, and particularly to evaluate and compare quantitatively the seismic risk between the PR and pipes, the piping system was designed according to this method.

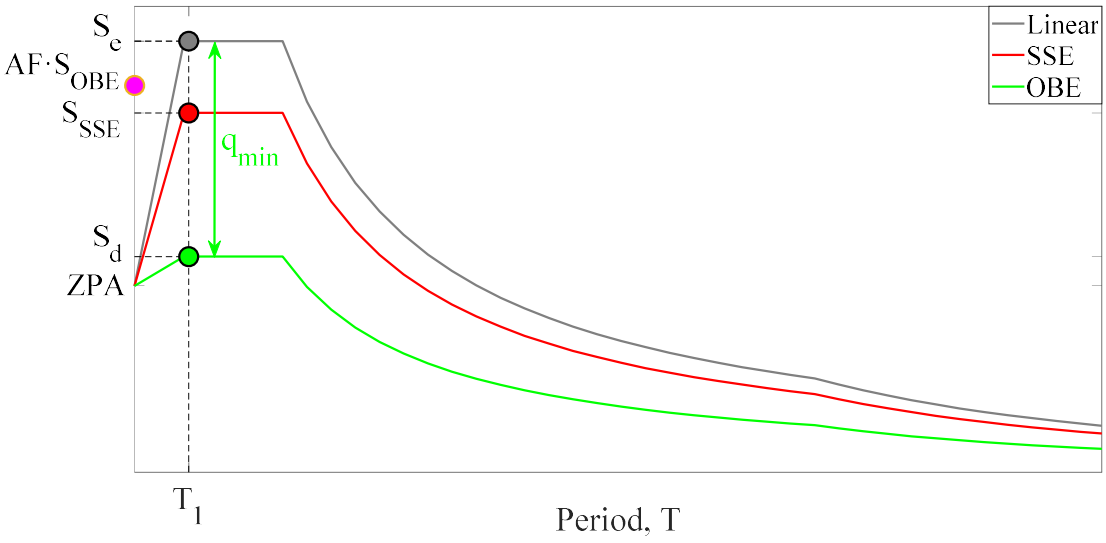

Fig. 4 The response spectra adopted for the design of pipe rack and pipelines (ZPA= zero period acceleration)

According to [7], the OBE acceleration (also called design basis acceleration), S_{OBE}, which is considered in this study equal to the design spectral acceleration, S_d, shall develop stress demand below the 80% of the yielding value accounting for the stress intensification factor of nonlinear pipe members. Also, the pipe stress shall not exceed by 20% the yielding stress for the SSE level, S_{SSE}, which is equal to $1.5 \cdot S_d$. It is emphasized that this seismic level is considered as an input at the PR base. The acceleration undergone by the piping is much greater, since they are designed for acceleration equal to $AF \cdot S_{OBE}$ (Fig. 4).

After scaling each record at the S_{OBE} level, the maximum Von Mises stress of pipes was evaluated at each pipe separately. The analysis showed that pipe 6 (or P-6) exceeded the code stress limit by 15% at PS4(6), and therefore the columns cross-section increased further. The final dimension of columns and beams was 700x700mm, 400x400mm (X-direction) and 400x600 mm (Y-direction), respectively. After PR stiffening, the elbow of P-1 was the most vulnerable pipe component. It is also worth mentioning that the differential displacement between the support PS3(6) (tank attachment point) and the support PS4(6) in the X direction, $DD\text{-}X_T$, increased due to the out-of-phase response of PR with the tank. On the other hand, the differential displacement of PS4(6) with the BC2(6), $DD\text{-}X_B$, was reduced, and thus the PR stiffening acted as a fuse for P-6. Finally, the differential displacement between the tank and the PR, $DD\text{-}Y_T$, rose mildly in the Y direction due to the stiffening. The seismic behaviour of pipes could be critical in both directions and complex depending on the differential displacements, internal and external, as well as rigidity of boundary conditions. This indicates that static analysis may not be always able to describe the complexity of the seismic response of these systems.

The maximum response of PR and piping during the design phase is quoted in Table 2. In this study, the exceedance of SLS for the PR is correlated with *IDR* equal to 0.60% ([25]). The *IDR*

was estimated roughly at 0.40% for both analysis types at S_e, which means that the SLS was not exceeded. The strain remained slightly below the yielding point on P-1 at S_{SSE}, and surely, the high rigidity of the PR was the main reason for this behaviour. The response spectrum method resulted in 48% smaller stress at S_{OBE} and also underestimated considerably the *PFA*, thus this method may not be always acceptable for the analysis of these systems. The *AF* using as a reference the Peak Ground Acceleration (*PGA*) was estimated at 2.54 out of the three records, which is almost 1.58 and 1.08 times smaller than the limit values in [9] and [6], respectively (a_p=5 given that T_1<*0.5 sec*). The mild difference of AF compared with [6] confirms the outcome of [11] and [10] that the code gives a good approximation of the peak floor acceleration for periods sufficiently larger or smaller than the fundamental period. Last but not least, the maximum differential displacement in X and Y direction is quoted in Table 4, since it was the governing reason of pipe failure.

Table 2: Maximum response of the system at S_{OBE} seismic level

	Response spectrum	Time history
IDR (%)	0.20	0.18
Pipe stress (MPa)	104	153
	120	230
PFA/PGA	1.04	2.54
(DD-X, DD-Y) (mm)	N.A.	(21.10, 20.16)

3. Seismic risk assessment

The seismic assessment can give a better insight of the seismic risk of a code-conforming PR coupled with piping. The selection of a suitable analysis software is a top priority and should rely upon the model requirements e.g. description of material nonlinearity and nonlinear geometry of pipe bend that should be able to capture the ovalisation and warping phenomena. In the framework of this study, the advanced simulation platform ABAQUS [21] is selected not only for describing the nonlinear response of pipes but also of concrete members in a robust manner. The scale of the RC PR model is not large; however, the consideration of the tank due to dynamic coupling effects makes the use of a narrow-range method more suitable. Such a decision becomes even more demanding when concrete members are analysed rigorously on ABAQUS due to the capabilities of the software for concrete material description. To this effect, the time-efficient cloud analysis method is selected, as described in the following, to examine the efficiency and sufficiency of tested IMs as well as the seismic risk of the system.

3.1 Analysis of numerical model on ABAQUS

The structural members are modelled as C3D8R solid elements with a continuum, plasticity-based, damage model of concrete which assumes two failure mechanisms, viz tensile cracking and compressive crushing. After performing a mesh convergence study, the mesh density was selected smaller than 150 mm for all concrete members. Also, the size varied between 12mm and 48mm for the pipe bends and rose up to 150 mm for the straight ones. The material was assumed as elastic-perfectly plastic with 48MPa mean compressive strength (tensile the $1/10^{th}$ of the compressive) to reduce the computational cost, given that the main focus of the analysis will be on the pipes on which most of the damage is expected, as shown in the previous section. The

reinforcement yielding strength is equal to 575 MPa and was embedded into the concrete, albeit bond slip and dowel action were neglected. Finally, the straight pipes were modelled with beam elements B31, whereas 20 special purpose elements ELBOW32 were found enough to describe the behaviour of pipe bend. The pipe was made of A312/TP304L material with 277 MPa and 352 MPa yielding and ultimate strength, respectively, with 0.75% strain hardening parameter. The seismic combination that accounts for the temperature effects on piping was adopted during the assessment, as mentioned previously. Finally, it should be noted that the implicit scheme was used for the dynamic analysis of the system by virtue of its efficiency in solving problems with material and geometrical nonlinearity. The final model for seismic assessment is shown in Fig. 5.

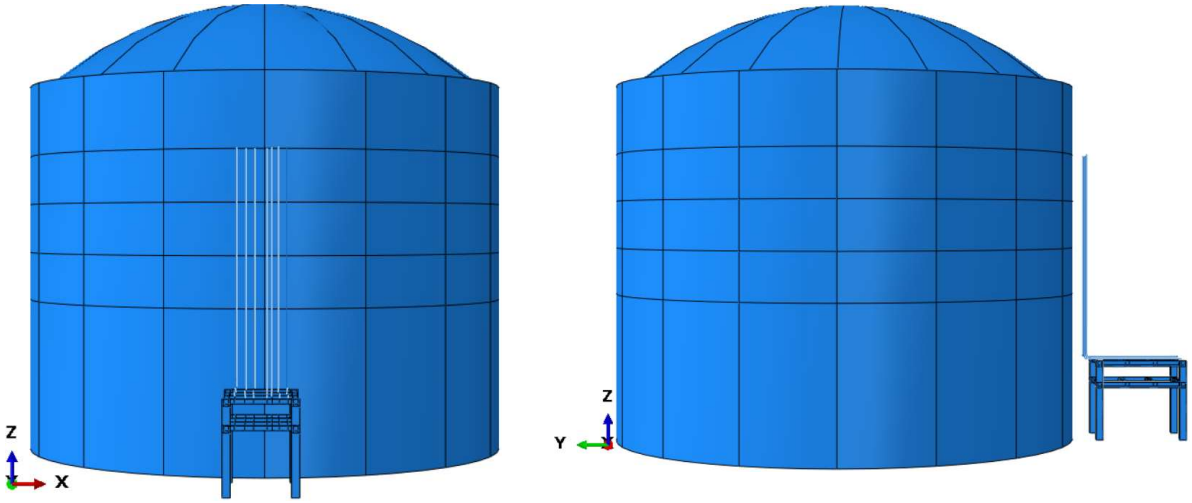

a) b)

Fig. 5 The numerical model under consideration in a. x-z and b. y-z plane on [21]

3.2 Seismic ground motions

The seismic demand of the PR and pipes is obtained from inelastic response history analyses, performed using 20 natural and spectrum compatible ground motions according to [6]. The

Uniform Hazard Spectrum (UHS) approach accounts for the envelope of spectra corresponding to different seismic sources, and the pipe rack – piping systems usually have more than one mode of interest; therefore, the selection of this method can be safer compared to conditional mean spectrum that has been found to underestimate the risk at periods other than the conditioning one ([26]). The UHS approach requires that the target average spectrum of selected records should not be less than the 90% of target spectrum within the $[0.2 \cdot T_1, 2 \cdot T_1]$ period range, where T_1(=0.24sec) is the fundamental period of the structure in the weakest (Y) direction. Due to the mild difference between the principal period in X and Y direction (T_X= 0.25 sec), the compatibility applies also to the X direction with a good approximation. It is noted that the code does not specify any upper bound of the average spectrum, but 30% limit is commonly adopted. The spectrum compatible ground motions refer both to near- and far-field conditions, epicentral distance, *R*, from 5 to 100 kms, magnitude, M_W, from 5.3 to 6.9, soil type C and shear wave velocity, $V_{s,30}$, between 180 and 360 m/s [6]. The *PGA* varies from 0.041 g to 0.509 g, and the Peak Ground Velocity (*PGV*) fluctuates from 2.3 cm/s to 35.4 cm/s. The records were shortened so that the acceleration spectrum does not change within the specified period range (bracketed duration). The response spectra of the records along with the bounds and period range are shown in Fig 6.

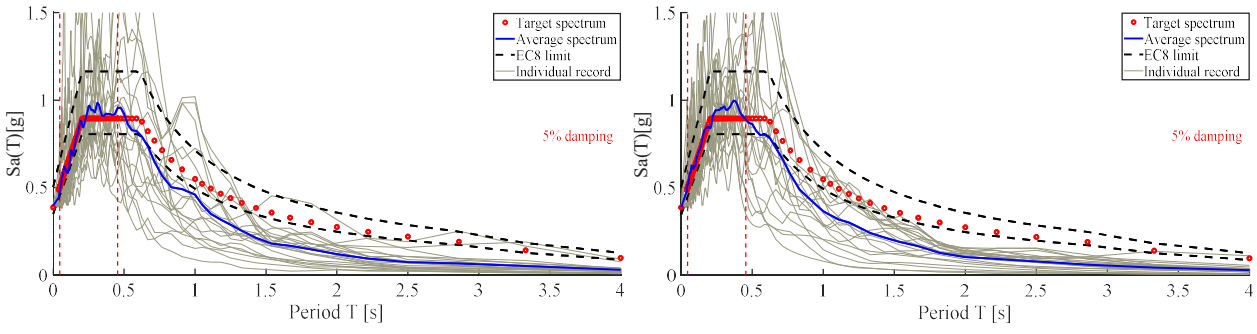

Fig. 6 The 20 spectrum compatible records in the a. X and b. Y direction according to [6]

3.3 Preliminary analyses

The determination of acceptance criteria of PR and pipes is an important step for the seismic fragility assessment. The maximum drift ratio, *IDR*, is selected as the Engineering Demand Parameter (EDP) for the PR, because it is closely related to the global response of PR and pipes that should be evaluated as a system in the immediate aftermath of an earthquake event. Another parameter could be the plastic deformation on PR, though it refers to member level, and thus cannot be correlated effectively with the response of pipes, which does not necessarily mean that repair of structural members is not required. The lower threshold value of *IDR* for the SLS and SLLS is considered equal to 0.60% and 1.2%, respectively ([25]).

Concerning the acceptance criteria of pipes, there are three main failure modes, viz failure under tension, compression (local buckling) and fatigue. Although the last mode has been reported as equally crucial for pipes ([27]), only the first two modes were examined in this case study. The fatigue failure mode is correlated with the buckled area of pipe due to compressive strain and occurs due to strong repeated loading in that area after reaching the ultimate resistance. The SLLS is correlated with the exceedance of compressive strain resistance, ε_{Cu}, as defined in [27]. Also, the exceedance of ultimate compressive strain ε'_{Cu} is correlated with the collapse limit state. However, the ε'_{Cu} is not well defined and is based on engineering judgement. It should be taken into account that a pipe with strain quite larger than ε_{Cu} starts to be buckled and needs replacement even if no loss of containment occurs. Therefore, keeping the compressive strain as close as possible to ε_{Cu} e.g. up to two times greater, the fatigue phenomenon is not critical. Furthemore, the exceedance of SLLS for the pipe under tension was correlated with 0.5% strain ([27]). To simplify the forencic investigation of a limit state exceedance and stay on the safe side at the same time, the minimum between the tensional and compressive strain was considered by using the

scalar variable *PEMAG* (plastic magnitude) on ABAQUS. For the sake of completeness, the plastic strain ε_{Cu} is quoted in Table 3.

Table 3: The compressive strain resistance, ε_{Cu}, related to the SLLS of 7 pipes

ID	P1	P2	P3	P4	P5	P6	P7
SLLS	0.34%	0.52%	1.08%	0.76%	0.46%	0.61%	0.76%

Initially, a number of 7 spectrum compatible records , which is the minimum number for nonlinear analysis according to [6], were selected to investigate the response of PR – piping system at a preliminary stage. During the design phase, the pipes were more fragile than the PR given that they reached the yielding point, whilst the *IDR* was not greater than 0.40% at S_{SSE} seismic level. However, it still remains to be examined the seismic response considering more advanced concrete and pipe modelling, which might direct the subsequent steps of fragility analysis in a more efficient way given the high computational cost. The plastic deformation of PR under two seismic excitations, which were scaled at $S_e(T_1)$, $1.5 \cdot S_e(T_1)$ and $2.2 \cdot S_e(T_1)$ so that the PR reaches the SLS, is shown in Figs. 7a&b (the rest of records are not presented for brevity, since similar results can be drawn). The maximum plastic strain was observed either on the upper (Fig. 7a) or intermediate floor (Fig. 7b), which indicates that the pipes did not affect considerably the response of PR due to the flexible mechanism of pipe-to-pipe support connection. Also, the development of equivalent plastic strain due to compression (*PEEQ*) and tension (*PEEQT*) on PR is illustrated in Fig. 7a&b, respectively. The most intriguing remark pertains to the exceedance of crushing strain of 0.35% at $1.5 \cdot S_e(T_1)$ and $2.2 \cdot S_e(T_1)$, despite the fact that the *IDR* was close to the SLS at the same seismic level. The rather low value of *IDR* (global level) compared to the high plastic deformation, *PEEQ*, (local level) proves that the former EDP is more appropriate than the latter given that the PR is still able to carry the load of pipes.

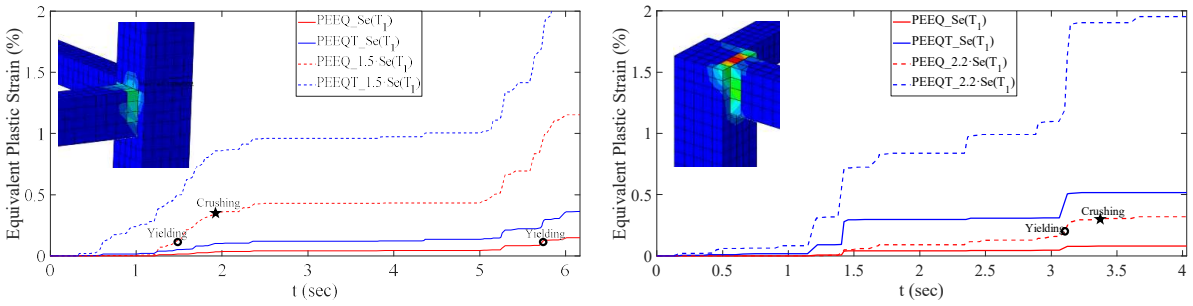

a) b)

Fig. 7. The development of maximum compressive, *PEEQ*, and tensile, *PEEQT*, strain at a. the top and b. intermediate floor for two seismic levels under Rec1 and Rec2, respectively.

The pipe 1 was the most vulnerable due to the high inertia effects in the Y direction. The pipe yielded at intensity close to the $S_e(T_1)$, as it was also observed during the design phase, and the total axial strain level, e, soared at 3.39 and 4.74 times the yielding value, e_y, at the higher seismic levels (Fig. 8a&b). Both strain levels corresponded to SLLS, albeit the PR was at SLS. This seismic response was expected, since the pipe was flexibly supported and the PR was quite rigid due to the strict design acceptance criteria that were highlighted during the design phase. The maximum differential displacement between the rack and the adjacent tank is also quoted along with the time of occurrence. It is noteworthy that the differential displacement was not always sychronised with the maximum strain, particularly at high seismic intensity. For example, the maximum axial strain, *e,* occurred mildly later than 6.00 sec, whilst the maximum *DD-*Y_T appeared at 6.00 sec and 4.63 sec for the Rec1 at $S_e(T_1)$ and $1.5 \cdot S_e(T_1)$, as shown in Fig. 8a, which singifies the complexity of response and the influence of internal pipe supports and boundary conditions.

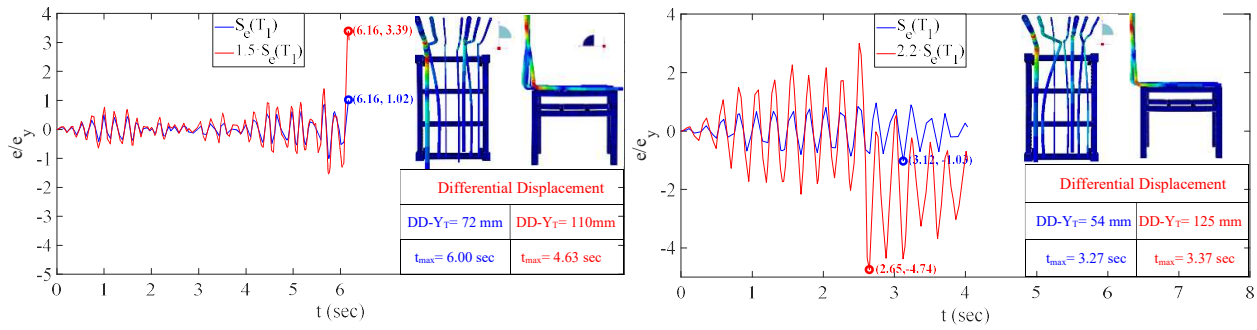

a) b)

Fig. 8 The time history of total axial strain *e* under a. Rec1 and b. Rec2 seismic excitation. The strain distribution as well as the maximum differential displacement and the time of occurrence are also quoted.

3.4 Cloud analysis

Numerous nonlinear dynamic analysis procedures exist in the literature for characterizing the relationship between an EDP and IM ([28]). Cloud analysis is a short range, efficient and simple in implementation method, which is proposed in the context of SAC-FEMA formulation ([29]). The cloud method is adopted in the framework of this study for two main reasons; first, the model is rigorous and the scale is quite large, thus a time efficient method could significantly reduce the computational cost; secondly, only the exceedance of SLLS is of concern, particularly for the pipes that have been found more fragile.

The main shortcomings of the method regard the assumption of the constant conditional standard deviation for the distribution of EDP given an IM and the strong dependence on the number and type of records. Strictly speaking, the dispersion of EDP may increase at higher IM levels, as it was observed in [30]; however, only the SLLS is considered for the pipes, thus this shortcoming does not affect considerably the efficacy of the results of this study. Additionally,

[31] proposes that at least 30% of the selected records should exceed the target performance level, so no extrapolation of regression line is required. This may require adjustments in the selection or scaling of records, as it was adopted in the following case-study. With regard to the second drawback, [31] recommends also that a wide range of spectral acceleration values should be selected towards reducing the standard error of the regression slope in the logarithmic scale. To make clear the confidence interval of seismic intensity on fragility functions, the standard error is evaluated as a percentage of median intensity.

3.4.1 Response Statistics

The probabilistic estimation of EDP, and that is the plastic strain, PEMAG, for pipes and *IDR* for PR given an IM is attained through the least sum of the squares of the residual method. Since the logarithmic distribution has been found to describe better the structural demand-seismic intensity relation, a probabilistic model of logarithmic linear regression is considered. The following properties characterise the logarithmic linear regression:

$$EDP = (a \cdot IM^b) \cdot \varepsilon$$
$$\mu_\varepsilon = 1 \;\&\; \sigma_{ln\varepsilon} = \beta_{EDP|IM} \tag{2}$$

where a is a parameter and b is the slope in log-space. The lognormal random variable ε has median, μ_ε, equal to unity and its logarithmic standard deviation, $\sigma_{ln\varepsilon}$, is equal to the standard deviation of the ln of EDP for a given value of IM, $\beta_{EDP|IM}$ (eq.2). The latter constitutes a metric of the efficiency of the regression of tested IMs to describe the seismic response (or EDP) of a structure. Lower $\beta_{EDP|IM}$ values indicate reduced dispersion around the median or in other words a more efficient IM.

$$(\ln EDP|IM) = \mu_{\ln EDP|IM} = \ln \eta_{EDP|IM} = \ln a + b \cdot \ln IM$$
$$\sqrt{VAR(EDP|IM)} = \sigma_{lnEDP|IM} \triangleq \beta_{lnEDP|IM} = const \quad (3)$$

Assuming that the EDP follows a logarithmic standard distribution for a given IM, the logarithm of the median is equal to the mean of the logarithm of EDP. The variance (*VAR*) or the squared standard deviation of the logarithm of EDP, $\sigma_{lnEDP|IM}$, is equal with the dispersion of EDP, $\beta_{lnEDP|IM}$ (eq. 3). Therefore, the parameters of the linear regression, a and b, can be obtained by estimating the $\mu_{lnEDP|IM}$, using linear regression in the logarithmic space of "cloud" data. The cumulative lognormal distribution of the observed data is expressed by:

$$P[EDP_D > EDP_C|IM] = \Phi\left(\frac{\ln(a \cdot IM^b) - \ln \eta_{EDP|IM}}{\beta^2_{EDP|IM}}\right) = \Phi\left(\frac{\ln(IM) - \ln \eta_{EDP|IM}}{\beta^2_{EDP|IM}/b}\right) \quad (4)$$

It is noted that the dispersion $\beta_{EDP|IM}$ accounts only for the record-to-record variability due to the limited research on the type of structure under consideration. Common values of modelling uncertainties as proposed e.g. in [32] for building structures and the assumption underlying the combination rule (total variance being the sum of variances) may not be totally valid for this system. Additionally, the efficiency of different IMs is examined in the following, thus examining other types of uncertainty may blur the comparison between them. The interested reader can find more information about epistemic and aleatory uncertainties in [32] and [33].

3.4.2 Efficiency of seismic IMs and fragility derivation

The term efficiency is used to express the ability of an IM to describe the structural response with low dispersion. The parameters that affect the efficiency of an IM regard the type of system e.g. regular or irregular, the level of nonlinearity as well as the EDP. Although the probabilistic seismic assessment of common building structures and bridges has been examined by employing peak ground or spectral measures to describe efficiently the seismic intensity ([16], [17], [34] and [35], among many others), the lack of literature for the assessment of pipes mounted on PRs makes the selection more challenging and still under investigation. Elevated pipes interact with supporting structures and adjacent ones, and they are affected by the type of supports and connection with equipment, exhibiting several governing vibration modes. Spectral IMs may be efficient to describe the seismic response of elevated pipes, though attention should be given to the fact that pipes are usually unrestrained in the longitudinal direction (slide support), and therefore partially independent from the rack-induced inertia.

In the framework of this study, the response of pipes is correlated with the spectral acceleration at the PR and most vulnerable pipe (P-1) fundamental period in the Y direction, $S_a(T_1=0.24\ sec)$ and $S_a(T_P=0.21\ sec)$, respectively, as well as $DD\text{-}Y_T$, PGV and Arias Intensity, I_A. The $DD\text{-}Y_T$ is used to illustrate the failure mode of pipes, given that it cannot be predicted by a ground motion prediction model. However, the DD-Y_T can be adopted as an estimate of piping damage inside critical process units towards reducing the response time e.g. for pipe valves closure. For example, (Luzi and Crosetto, 2015) introduced a terrestrial remote sensing technique, namely "real aperture radar interferometry", for measuring the displacement of various civil structures for structural health monitoring and early warning in the immediate aftermath of extreme events.

The linear regression lines of cloud data for the aforementioned IMs as a function of *PEMAG* are shown in Fig. 9a-e. The estimated spectral acceleration at the fundamental period of P-1 was mildly more efficient than the one at the fundamental period of the PR. The Arias Intensity, I_A, was proved the least efficient ($\beta_{PEMAG|DD\text{-}Y}=0.30$), although the difference with the S_a but also with the *PGV* was not substantial. Finally, the *DD-*Y_T was considerably more efficient than the rest of IMs, since the logarithmic standard deviation, $\beta_{PEMAG|DD\text{-}Y}$ did not exceed 0.13. This outcome is in agreement with the research of [15] who concluded that the differential displacement was the predominant failure mode of a nuclear piping system. In fact, the pipes are strongly influenced by the response of rigid storage tank, and this is the reason that ground measures were evaluated relatively efficient compared to spectral measures. In contrast, [37] illustrated that spectral measures expressed the piping response with lower dispersion because of the higher mode effects of a steel rack. Finally, it should be emphasized that the real-time measurement of DD-Y_T as part of an early warning system can be an effective method for accident prevention and consequence mitigation inside the process plant.

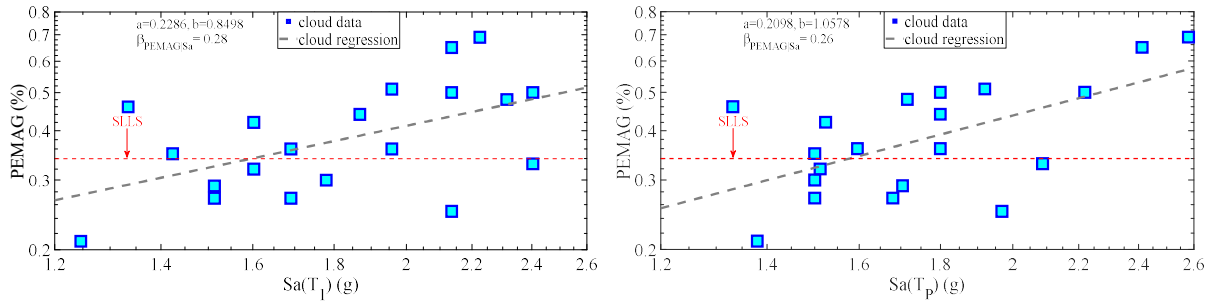

a) b)

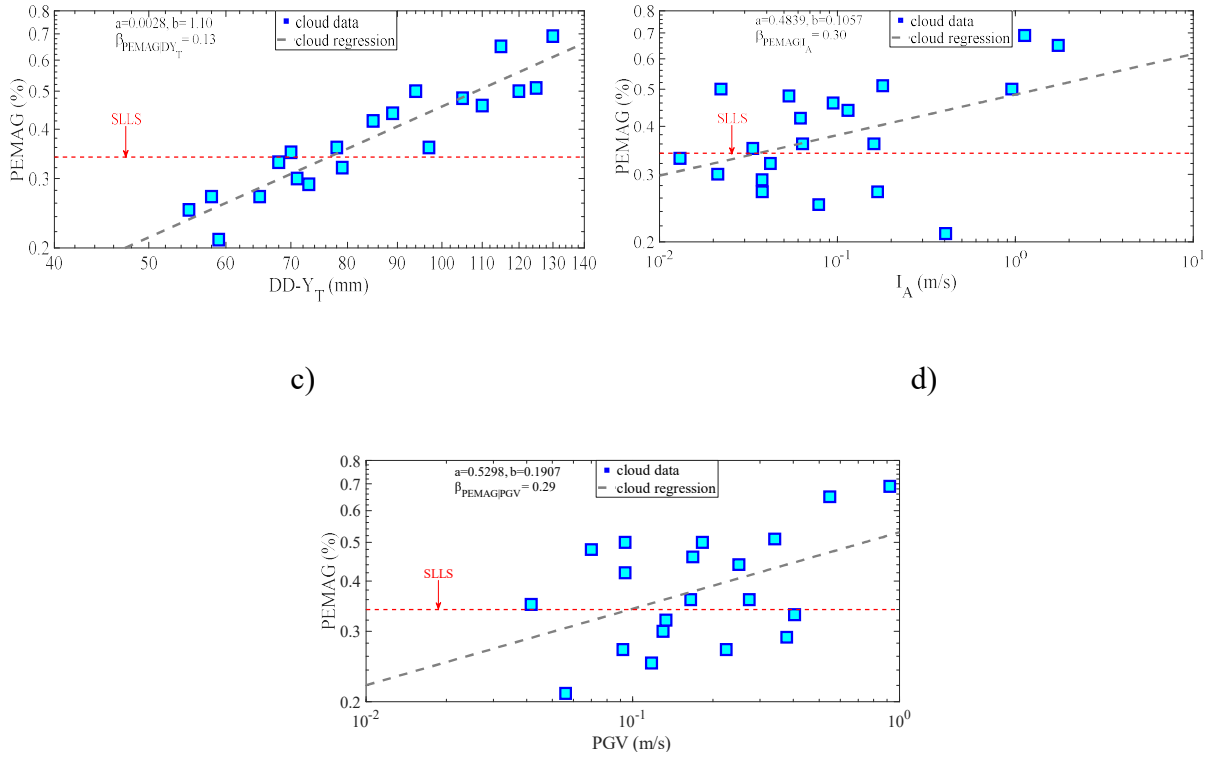

Fig. 9 Linear regression of pipelines for the SLLS accounting for different IMs, namely a. $Sa(T_1)$, b. $Sa(T_P)$ and c. DY_T, d. I_A and e. PGV

The fragility functions for the two spectral accelerations are plotted in Fig. 10a&b. As stated in [36] and [37], the median $\eta_{EDP|IM}$ is only an estimate of the "true" median value. Therefore, using another set of records, equal in number with the first one and equivalent in spectrum characteristics, the median will be different due to record randomness. The most efficient way to deal with this uncertainty is to increase significantly the number of records, which may not be feasible due to the excessive computational cost. Alternatively, the standard error of the mean can be used, in virtue of the limited number of records, that is equal to two times the standard deviation, $\beta_{EDP|IM}$, divided by the square root of number, N, of records. The standard error represents the

deviation of the sample mean around the true value and can further be used for illustrating the 95% Confidence Interval (CI).

The standard error as a percentage of the median was estimated at 11% and 13% for the $S_a(T_p)$ and $S_a(T_1)$, respectively. The median $S_a(T_1)$ and $S_a(T_p)$ was estimated roughly at 1.6g. During the design phase, the *DD-*Y_T was evaluated nearly 40 mm at S_d, whereas the median *DD-*Y_T rose at 76.5 mm for the SLLS. Finally, the observed *MAF (or* P_C*)* of exceedance of SLLS was estimated through the risk equation ([29] and eq. 4), integrating the fragility curve, P(·), with the hazard curve, H(·), of the site. The MAF was estimated for the piping based on spectral acceleration, $S_a(T_p)$, at $6.1 \cdot 10^{-4}$, which is considerably lower than the targeted value, $P_{a,C}$, of 0.0014. Based on the standard error, the upper value of risk rose by almost 34%.

$$MAF\ or\ \lambda_{LS} = -\int_0^{+\infty} P[EDP_D > EDP_C|IM] \cdot \frac{dH(IM)}{d(IM)} d(IM) \quad (5)$$

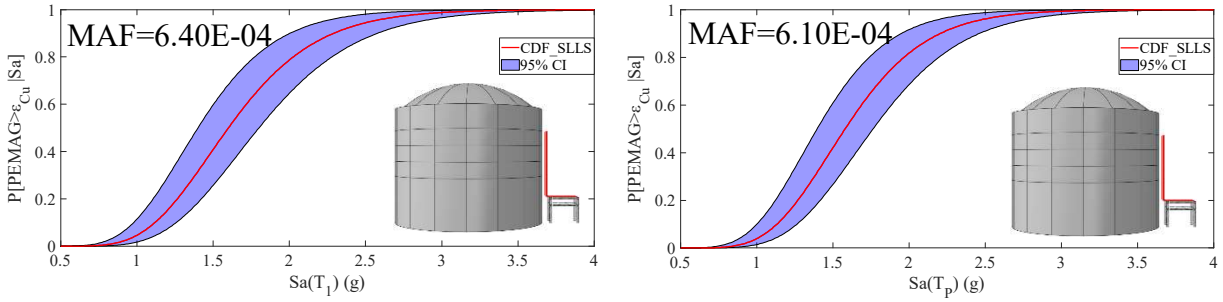

a) b)

Fig. 10 Fragility curves of pipelines for the SLLS accounting for a. $S_a(T_1)$ and b. $S_a(T_P)$

Furthermore, the seismic risk of the PR was also evaluated. The cloud regression of *PGA-IDR* and $S_a(T_1)$*-IDR* relation is illustrated in Fig. 11a&b. The difference in the logarithmic standard deviation was negligible between the two IMs, and the standard error as a percentage of the median

was roughly at 9%, which signifies that the PR did not experience considerable plastic deformation. [40] used two record sets to investigate the response of Italian code-conforming bared RC frames. The conditional spectrum records yielded $\beta_{IDR|Sa}$ close to the observed value in this study. Finally, the median was evaluated at 1.17g and 2.06g, as shown in Fig.11c&d, and the seismic risk was extremely low, since the MAF was equal to $3.36 \cdot 10^{-4}$ based on $S_a(T_1)$.

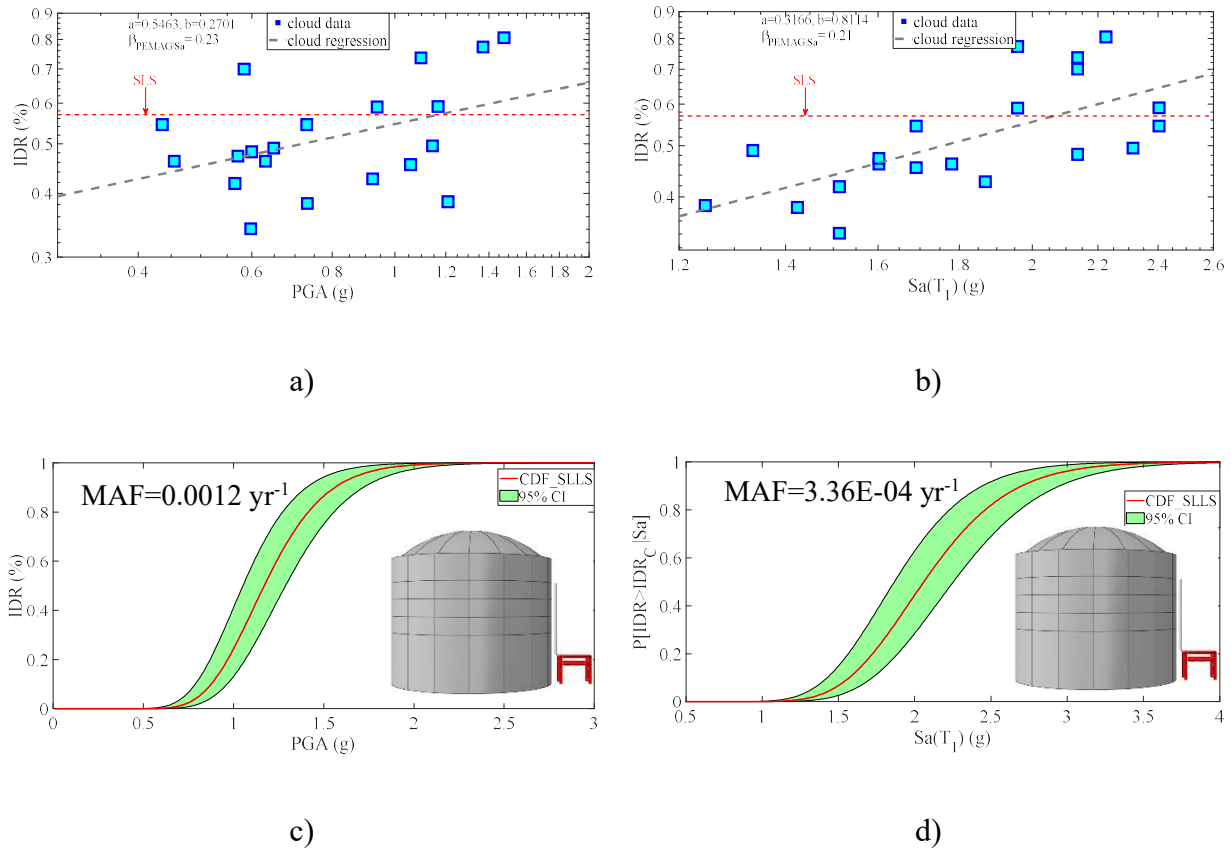

Fig. 11 Linear regression and fragility curves of PR for the SLLS accounting for a&b. *PGA* and c&d. $S_a(T_1)$ as IM

3.4.3 Sufficiency of seismic IMs

An IM is sufficient when it renders the EDP conditionally independent of seismological characteristics, such as the magnitude, M_W, and epicentral distance, R, ([41]). This means that there

is no need to condition the exceedance probability of a limit state on the aforementioned properties yet only on the IM. The sufficiency of an IM is evaluated using the p-value, which is defined as the probability of the null hypothesis, where the null hypothesis states that the coefficient of regression (β) is zero. If the p-value is smaller than a threshold value, which is commonly considered equal to 5%, then there is evidence for rejecting the null hypothesis (statistically significant coefficient of regression) and characterizing an IM as insufficient. The evaluation of IMs sufficiency was achieved by performing regression analyses on the residuals of plastic strain, *PEMAG*, and *IDR* with respect to magnitude and epicentral distance of the selected seismic records. The residuals $\varepsilon_{res|IM}$ were defined as the difference between the observed strain from the nonlinear analysis of pipes and the strain from the regression fit line that was defined previously for evaluating the efficiency of tested IMs. Fig. 12 demonstrates the two representative regression analyses of the residuals relative to the $S_a(T_P)$, which was the most efficient IM that can be used for risk estimation, as a function of magnitude, M_W, and epicentral distance, R.

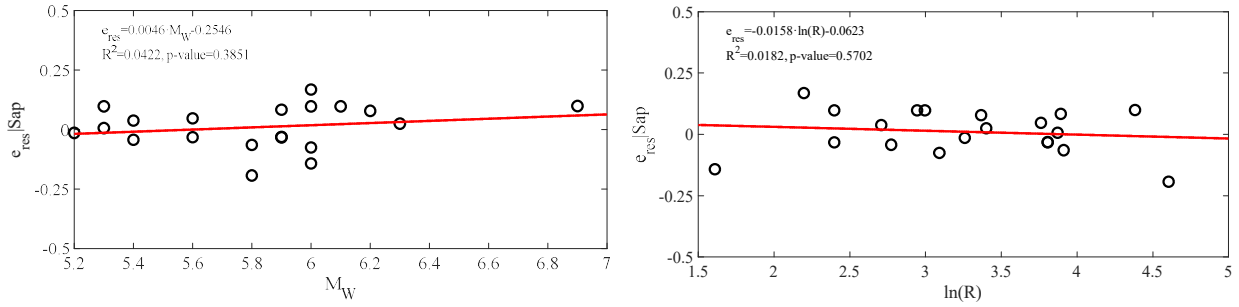

a) b)

Fig. 12 Representative regression analyses of $\varepsilon_{res|IM}$ relative to a. magnitude, M_W, and b. epicentral distance, *lnR*, of the selected ground motions towards evaluating the sufficiency of $S_a(T_P)$.

The logarithmic standard deviation, $\beta_{EDP|IM}$, and the p-value with respect to seismological variables of the tested IMs are quoted in Table 4. It is stressed out that all the IMs proved to be sufficient with respect to M_W and R. However, it should also be highlighted that, in case of pipes, the $S_a(T_P)$ was evaluated as more sufficient compared to ground measures. Therefore, the decision of using $S_a(T_P)$ for the estimation of risk is proved reasonable. Finally, it is highlighted that in contrast with underground pipelines that are described more efficiently and sufficiently by ground measures ([16]), spectral measures at different vibration periods should be adopted in case of process piping.

Table 4: Logarithmic standard deviation and the p-value of M_W and R for the tested IMs

		$\beta_{EDP\|IM}$	p-value (M_W, R)
Pipelines	DY_T	0.13	(0.4614, 0.4407)
	$Sa(T_1)$	0.28	(0.3382, 0.6250)
	$Sa(T_p)$	0.26	(0.3851, 0.5702)
	PGV	0.29	(0.2204, 0.2805)
	I_A	0.30	(0.1851, 0.3170)
Pipe rack	$Sa(T_1)$	0.21	(0.7315, 0.8577)
	PGA	0.23	(0.8424, 0.7310)

3.5 Evaluation of amplification factor

As mentioned above, the equivalent static methodology is usually adopted in the industrial sector for evaluating the seismic response at pipe's level. Also, it might be the case that the design of pipes precedes the design of the PR, thus the relative ratio between the two periods is not taken into account (see eq.1). In that case, the *PGA* of the design spectrum is used, and the ratio of the periods is considered equal to unity for conservativeness. To evaluate this assumption, the ratio of *PFA* with the *PGA* was estimated for the selected records, as shown in Fig. 14a. Apart from the rigid PR that was assessed previously, a flexible yet code-conforming PR, which was examined during the design phase, was also considered for comparison purposes. The flexible PR caused slightly greater *PFA*; nevertheless, attention should be drawn to the relatively close approximation of EC8 low limit vis-à-vis the average *AF* derived from the dynamic analyses (roughly 12% overestimated). On the other hand, NTC presented 1.6 times greater *AF* than the average. To examine further the *AF*, the spectral acceleration at the fundamental period of the most vulnerable pipe, P-1, was investigated, which is arguably more accurate than the previous approach (Fig. 13b). In contrast with the previous case, the EC8 limit underestimated the *AF* by almost 30%. Anew, this outcome comes in unison with the study of [11] and [42] who concluded that the acceleration is considerably underestimated at a period range in the vicinity of principal period of a structure. Thus, when a piping engineer selects this code and the spectral acceleration for the design of pipelines, the seismic demand could be underestimated. On the other hand, NTC overestimated by almost 60% the *AF*, which questions the use of the code for nonstructural components like pipes. Finally, it is noted that [7] proposes *AF* equal to 1.5, which is substantially lower compared to the average *AF*.

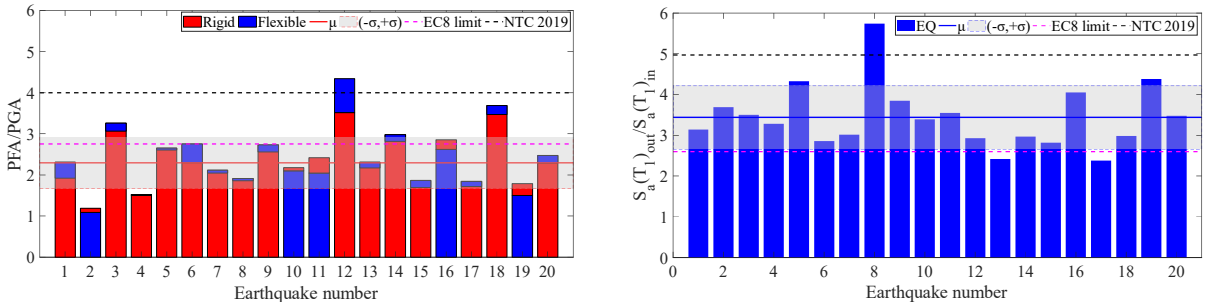

a) b)

Fig. 13 Amplification factors of seismic input at pipe's level considering a. *PGA* for the flexible and rigid PR and b. spectral acceleration, S_a, at P-1 fundamental period (the nominator and denominator on the ordinate regard the output and input of seismic motion)

4. Discussion and conclusions

The present study addressed the design and performance-based assessment of a typical RC pipe rack accounting for dynamic coupling with several steel pipes. The design of the system revealed that seismic code provisions might require the increase of pipe rack cross section to keep the piping in the elastic region. Also, the pipes were found vulnerable in both directions (transverse and longitudinal) during the design phase in virtue of differential displacement with the adjacent tank. The outcomes of the assessment are recapitulated as follows:

- Pipes were more vulnerable than the pipe rack and the mean annual frequency, *MAF*, of collapse for the pipes was estimated at 2.25 times lower than the target probability of exceedance given the spectral acceleration, $S_a(T_1)$, as IM. The seismic risk was almost 34% greater at the upper 95% confidence level.

- The spectral acceleration, S_a, was evaluated as an efficient and sufficient IM to describe the damage on pipes and was used for the risk estimation. The dispersion, $\beta_{PEMAG|Sa}$, was equal to 0.26, which is mildly smaller than the peak ground measures.
- The differential displacement, *DD-*Y_T, was illustrated to be the main failure mode of pipes at the intersection of pipe rack with the tank. The very low dispersion of *DD-*Y_T and the mild difference of dispersion between the spectral and peak ground measures indicate that the response was mainly governed by the interaction with the tank. Also, the inconsistency between the max DD-Y_T and pipe strain clearly shows that the response can become complex due to the interaction with the tank and internal supports.
- The pipe rack was quite stiff with very low *MAF* of exceedance even for the SLS. The high rigidity of the rack was derived by the demand of pipes to remain in the elastic range.
- The evaluation of amplification factor, *AF*, illustrated that EC8 and NTC seismic codes are inconsistent, and the *AF* should preferably be based on spectral acceleration to account for the dynamic characteristics of multiply-supported pipes. In that case, however, the AF was underestimated by almost 30% by EC8, whereas the NTC considerably overestimated the *AF*.

On a concluding note, the risk-inconsistency between the pipe rack and piping clearly urges for the use of performance design criteria for the dynamic coupled system, accounting for the inelastic deformation of pipe material and component damping. This is issue is investigated by the Authors. Also, the measurement of differential displacement for reducing the response time and prioritising

actions in the aftermath of a severe event or the adoption of flexible pipe connection at the tank – rack intersection should be considered in the future.

List of abbreviations

AF = Amplification factor

BC = Boundary Condition

DD = Differential displacement

EDP = Engineering demand parameter

IM = Intensity measure

NPS = Nominal pipe size

OBE = Operating basis earthquake

PR = Pipe rack

PS = Pipe support

RC = Reinforced concrete

SLS = Serviceability limit state

SLLS = Safe-life limit state

SSE = Safe-shut down earthquake

Declaration of competing interest

The Authors declare no conflict of interest.

Acknowledgements

The work presented herein has received funding from the European Union's Horizon 2020 research and innovation programme under the Marie Sklodowska-Curie grant agreement No 721816. This support is gratefully acknowledged.

References

[1] E. Krausmann and A. M. Cruz, "Impact of the 11 March 2011, Great East Japan earthquake and tsunami on the chemical industry," *Nat. Hazards*, 2013.

[2] M. Eli, S. Sommer, T. Roche, and K. Merz, "The January 17,1994 Northridge Earthquake: Effects on Selected Industrial Facilities and Lifelines," 1995.

[3] K. Kidam and M. Hurme, "Analysis of equipment failures as contributors to chemical process accidents," *Process Saf. Environ. Prot.*, vol. 91, no. 1–2, pp. 61–78, Jan. 2013.

[4] M. Campedel, "Analysis of Major Industrial Accidents Triggered by Natural Events Reported In the Principal Available Chemical Accident Databases," 2008.

[5] E. Krausmann, A. M. Cruz, and B. Affeltranger, "The impact of the 12 May 2008 Wenchuan earthquake on industrial facilities," *J. Loss Prev. Process Ind.*, 2010.

[6] EN1998-1, *Eurocode 8: Design of structures for earthquake resistance - Part 1 : General rules, seismic actions and rules for buildings*, vol. 1, no. English. 2004.

[7] EN13480-3, "EN 13480-3, 2002, Metallic Industrial Piping–Part 3: Design and Calculation, CEN, Brussels.," 2012.

[8] NTC, *"Norme Tecniche per le costruzioni", DM Infrastructure, 14 January*. (in Italian), 2018.

[9] NTC-N.7, *Circolare 21 gennaio 2019 n.7 " Istruzioni per l'applicazione dell'«Aggiornamento delle*

"Norme tecniche per le costruzioni"» di cui al decreto ministeriale 17 gennaio 2018". 2019.

[10] T. J. Sullivan, P. M. Calvi, and R. Nascimbene, "Towards improved floor spectra estimates for seismic design," *Earthq. Struct.*, 2013.

[11] C. Petrone, G. Magliulo, and G. Manfredi, "Seismic demand on light acceleration-sensitive nonstructural components in European reinforced concrete buildings," *Earthq. Eng. Struct. Dyn.*, 2015.

[12] O. S. Bursi, F. Paolacci, M. S. Reza, S. Alessandri, and N. Tondini, "Seismic Assessment of Petrochemical Piping Systems Using a Performance-Based Approach," *J. Press. Vessel Technol. Trans. ASME*, vol. 138, no. 3, 2016.

[13] L. Di Sarno and G. Karagiannakis, "Petrochemical Steel Pipe Rack: Critical Assessment of Existing Design Code Provisions and a Case Study," *Int. J. Steel Struct.*, Sep. 2019.

[14] A. A. D. L. Di Roseto, A. Palmeri, and A. G. A. G. Gibb, "Performance-based seismic design of a modular pipe-rack," *Procedia Eng.*, vol. 199, pp. 3564–3569, 2017.

[15] E. Salimi Firoozabad, B. G. Jeon, H. S. Choi, and N. S. Kim, "Seismic fragility analysis of seismically isolated nuclear power plants piping system," *Nucl. Eng. Des.*, 2015.

[16] G. Tsinidis, L. Di Sarno, A. Sextos, and P. Furtner, "Optimal intensity measures for the structural assessment of buried steel natural gas pipelines due to seismically-induced axial compression at geotechnical discontinuities," *Soil Dyn. Earthq. Eng.*, 2020.

[17] R. Maio and G. Tsionis, "Seismic fragility curves for the European building stock: Review and evaluation of analytical fragility curves," 2016.

[18] G. Karagiannakis, L. Di Sarno, J. Žižmond, and M. Dolšek, "Seismic design and assessment of risk-targeted reduction factor for a reinforced concrete pipe rack – piping system," in *17th World Conference on Earthquake Engineering, 17WCEE Sendai, Japan - September 13th to 18th 2020*,

2020, pp. 1–12.

[19] EN1998-4, *Design of structures for earthquake resistance – Part 4: Silos, tanks and pipelines [Authority: The European Union Per Regulation 305/2011, Directive 98/34/EC, Directive 2004/18/EC]*. 2006.

[20] EN 1998-4, *Design of Structures for Earthquake Resistance-Part 4: Silos, Tanks and Pipelines*, vol. 1. 2004.

[21] ABAQUS, "ABAQUS 6.17 Analysis User's Manual'. Online Documentation Help: Dassault Systèmes.," 2017.

[22] G. E. Varelis, S. A. Karamanos, and A. M. Gresnigt, "Pipe Elbows Under Strong Cyclic Loading," in *Proceedings of the ASME 2012 Pressure Vessels & Piping Conference, Toronto, Orario, Canada*, 2012, vol. 135, no. July 15-19, p. 45.

[23] L. Di Sarno and G. Karagiannakis, "On the seismic fragility of pipe rack—piping systems considering soil–structure interaction," *Bull. Earthq. Eng.*, Feb. 2020.

[24] M. Farhan and S. Bousias, "Seismic fragility analysis of LNG sub-plant accounting for component dynamic interaction," *Bull. Earthq. Eng.*, 2020.

[25] A. S. Elnashai and L. Di Sarno, *Fundamentals of Earthquake Engineering: From Source to Fragility*, Second. Wiley, 2015.

[26] T. Lin, C. B. Haselton, and J. W. Baker, "Conditional spectrum-based ground motion selection. Part II: Intensity-based assessments and evaluation of alternative target spectra," *Earthq. Eng. Struct. Dyn.*, 2013.

[27] M. Vathi, S. A. Karamanos, I. A. Kapogiannis, and K. V. Spiliopoulos, "Performance criteria for liquid storage tanks and piping systems subjected to seismic loading," *J. Press. Vessel Technol.*, 2017.

[28] K. Bakalis and D. Vamvatsikos, “Seismic Fragility Functions via Nonlinear Response History Analysis,” *J. Struct. Eng. (United States)*, 2018.

[29] C. A. Cornell, F. Jalayer, R. O. Hamburger, and D. A. Foutch, “Probabilistic Basis for 2000 SAC Federal Emergency Management Agency Steel Moment Frame Guidelines,” *J. Struct. Eng.*, 2002.

[30] D. Vamvatsikos and C. Allin Cornell, “Incremental dynamic analysis,” *Earthq. Eng. Struct. Dyn.*, vol. 31, no. 3, pp. 491–514, 2002.

[31] F. Jalayer, H. Ebrahimian, A. Miano, G. Manfredi, and H. Sezen, “Analytical fragility assessment using unscaled ground motion records,” *Earthq. Eng. Struct. Dyn.*, 2017.

[32] HAZUS-MH MR5, “Multi-hazard Loss Estimation Methodology Earthquake Model,” 2010.

[33] D. Vamvatsikos and M. Fragiadakis, “Incremental dynamic analysis for estimating seismic performance sensitivity and uncertainty,” *Earthq. Eng. Struct. Dyn.*, vol. 39, no. 2, pp. 141–163, 2010.

[34] M. Dolsek, “Incremental dynamic analysis with consideration of modeling uncertainties,” *Earthq. Eng. Struct. Dyn.*, vol. 38, no. 6, pp. 805–825, 2009.

[35] J. E. Padgett, B. G. Nielson, and R. DesRoches, “Selection of optimal intensity measures in probabilistic seismic demand models of highway bridge portfolios,” *Earthq. Eng. Struct. Dyn.*, 2008.

[36] D. Vamvatsikos and C. A. Cornell, “Developing efficient scalar and vector intensity measures for IDA capacity estimation by incorporating elastic spectral shape information,” *Earthq. Eng. Struct. Dyn.*, 2005.

[37] L. Di Sarno and G. Karagiannakis, “Seismic Assessment of Pipe Racks Accounting for Soil-Structure Interaction,” *Int. J. Steel Struct.*, 2020.

[38] G. Baltzopoulos, R. Baraschino, and I. Iervolino, “On the number of records for structural risk estimation in PBEE,” *Earthq. Eng. Struct. Dyn.*, 2019.

[39] N. Shome and C. A. Cornell, “‘Probabilistic Seismic Demand Analysis of Nonlinear Structures’; Report No. RMS-35. Reliability of Marine Structures Program, Department of Civil and Environmental Engineering, Stanford University,” 1999.

[40] A. Suzuki and I. Iervolino, “Seismic Fragility of Code-conforming Italian Buildings Based on SDoF Approximation,” *J. Earthq. Eng.*, 2019.

[41] N. Luco and C. A. Cornell, “Structure-specific scalar intensity measures for near-source and ordinary earthquake ground motions,” *Earthq. Spectra*, 2007.

[42] R. J. Merino Vela, E. Brunesi, and R. Nascimbene, “Derivation of floor acceleration spectra for an industrial liquid tank supporting structure with braced frame systems,” *Eng. Struct.*, 2018.